

ExpansionNet v2: Block Static Expansion in fast end to end training for Image Captioning

Jia Cheng Hu¹, Roberto Cavicchioli¹, Alessandro Capotondi¹

¹University of Modena and Reggio Emilia
{name.surname}@unimore.it

Abstract

Expansion methods explore the possibility of performance bottlenecks in the input length in Deep Learning methods. In this work, we introduce the Block Static Expansion which distributes and processes the input over a heterogeneous and arbitrarily big collection of sequences characterized by a different length compared to the input one. Adopting this method we introduce a model called ExpansionNet v2, which is trained using our novel training strategy, designed to be not only effective but also 6 times faster compared to the standard approach of recent works in Image Captioning. The model achieves the state of art performance over the MS-COCO 2014 captioning challenge with a score of 143.7 CIDEr-D in the offline test split, 140.8 CIDEr-D in the online evaluation server and 72.9 All-CIDEr on the nocaps validation set. Source code available at: https://github.com/jchenghu/ExpansionNet_v2.

1 Introduction

Image Captioning describes the problem of generating a natural language description of an image without human intervention. It's a multi-modal problem that requires from the system both language comprehension and visual understanding. Over the past years, thanks to an easy access to a huge amount of data and the increasing affordability of massive parallel computational resources, neural networks became the currently most popular and most performing tools in many Computer Vision and Natural Language Processing related research field. Neural image captioning systems consist typically of an encoder responsible of extracting the visual information for the decoder which instead generates a linguistically acceptable description, at the early stages they mostly respectively consisted of CNN and recurrent layers [35, 3, 27] since for many years they were the most performing tools in many Computer Vision and Natural Language Processing tasks. In recent years however, transformer based models [29] gained momentum and it either replaced or merged with existing approaches further improving the effectiveness of captioning models [24, 14, 9, 23, 40, 17]. All encoders

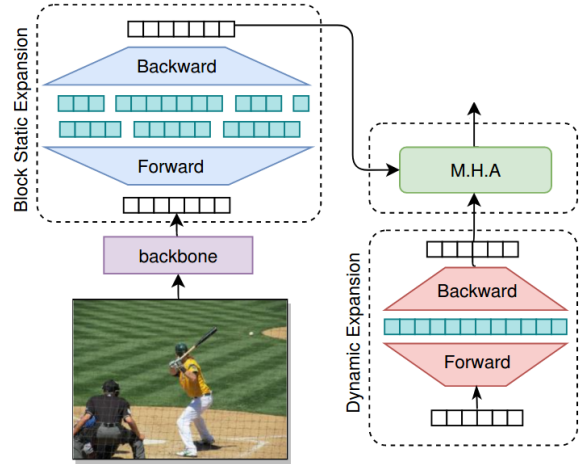


Figure 1: The expansion mechanism transform the input data into a new one featuring a different sequence length during the forward phase and performs the reverse operation in the backward pass in order to enable the network into processing the input unconstrained by the number of elements. The Block Static Expansion provides a way of performing these operations over a collection of arbitrary and diverse lengths at the same time.

until recent year relied on a convolutional backbone [31], an aspect that was changed in [33] which introduces the first fully attentive end to end architecture for Image Captioning, called PureT [33], enabled in particular by the Swin-Transformer [21]. Despite the impressive results of existing methods, in [11] we challenged the most popular approaches with the expansion layers, which consists of leveraging different sequence lengths compared to the one provided in the input. In this work we further explore the idea and improve the encoder by leveraging a set of multiple arbitrary sequence lengths, while preserving the efficiency of the original formulation. We design a training strategy that is not only effective but also several times faster than the standard one and we achieve the state of arts results on the MS-COCO 2014 challenge and competitive results on the nocaps validation set. The overall

contributions of this work are the following:

- a novel architecture for Image Captioning that achieves state of art performance in the popular MS-COCO 2014 challenge and competitive results on the validation nocaps dataset;
- the Block Static Expansion layer;
- a novel learning strategy that is more efficient and effective compared to the standard one, based upon an alternation of partial and end to end training, lowering the computational requirements of recent technologies in image captioning;

2 Related Works

Image Captioning models benefitted a lot from Deep Learning methods, from hand-crafted sentences aided by object detection systems [28, 37] they now consist of a neural encoder and decoder structure where the first is responsible of extracting meaningful visual information and the latter is responsible of generating the caption. The encoder in the early formulations consisted of a convolutional backbone [30, 35] but it was later replaced by an object detector [3] setting up a multi-modal sequence modeling problem over a position invariant collection of salient objects. Consequently, most of the methods, originally designed in the field of Natural Language Processing, could be adopted in Image Captioning as well, in particular, the works of [32, 3, 35, 30] relied on the Recurrent Neural Networks (RNNs) [6, 10], whereas most recent architectures exploited fully attentive models [9, 13, 24, 15, 40, 23]. The application of the Transformer has been proved to be surprisingly effective, despite the fact it was originally designed for the NLP field. However, due to the quadratic cost with respect to the input size, it couldn't easily replace the role of a convolutional backbone, in fact, from the sheer number of elements perspective images are typically orders of magnitude greater than text sequences, regardless of sub-word tokenization techniques. Despite the premise, the recent work of [21] introduced a fully attentive backbone for images and achieved state of art performances in many Vision related task and [33] proved it to be very effective in the Image Captioning as well. Additionally, in contrast to the previous captioning systems, [33] also provided the first end to end architecture achieving outstanding results at the cost of high computational requirements. Finally, in [11] we proposed an alternative method to the self-attention layer based upon the idea of changing the sequence length, in contrast to [7] however, we focused on the architectural front.

3 Method

3.1 Architecture

Our model consists of the standard encoder decoder structure implemented on top of the Swin-Transformer which details are provided in [21]. The image A , it is first fed into the backbone:

$$X_0 = \text{Swin-Transf}(A) \quad (1)$$

and generates the initial set of processed visual features $X_0 = \{x_1^0, x_2^0, \dots, x_N^0\}$, $x_i^0 \in \mathbb{R}^{d_m}$. The result is fed into the encoder which is made of N_{enc} Static Expansion \rightarrow FeedForward blocks, skip connection and pre-layer normalization [34] are adopted and the whole encoder is described by the following formulas for each $n = 1, \dots, N_{enc}$:

$$\begin{aligned} B_n &= X_{n-1} + \text{StaticExp}_n(\text{Norm}_n^{SE}(X_{n-1})) \\ X_n &= B_n + \text{FF}_n(\text{Norm}_n^{FF}(B_n)) \end{aligned} \quad (2)$$

Similarly, given $Y_0 = \{y_1^0, y_2^0, \dots, y_M^0\}$, $y_i^0 \in \mathbb{R}^{d_m}$ is the generic input sequence (during training stage so we can omit the time axis), the decoder is made of N_{dec} Dynamic Expansion \rightarrow Cross-Attention \rightarrow FeedForward blocks, skip connection and normalization is applied on each component. Each layer $n = 1, \dots, N_{dec}$ are described by the following equations:

$$\begin{aligned} B_n &= Y_{n-1} + \text{DynamicExp}_n(\text{Norm}_n^{DE}(Y_{n-1})) \\ W_n &= B_n + \text{Attention}_n(\text{Norm}_n^{CA}(B_n), X_{N_{enc}}) \\ Y_n &= W_n + \text{FF}_n(\text{Norm}_n^{FF}(W_n)) \end{aligned} \quad (3)$$

where the final output Y_n is fed to the classification layer. A visual representation of the architecture's main components is depicted in Figure 2.

3.2 Block Static and Dynamic Expansion Layers

The attention mechanism [4, 22] was first introduced to spread the input information throughout all encoder hidden vectors. In [11] instead we explored the idea of distributing the input content over an arbitrary number of elements. In its essence the expansion principle consists of transforming the input sequence into another one featuring a different length by means a "Forward expansion" and retrieving the original length back in the complementary backward operation. In particular two versions currently exist, called Static Expansion and Dynamic Expansion according to the nature of the transformation. The latter is designed to preserve the auto-regression property whereas the first can be operated in both bidirectional processing and decoding stage. The main differences lies in how the forward operation is performed, in particular, in the vector generation phase. In the Static Expansion case the expansion coefficient N_E defines the final size of

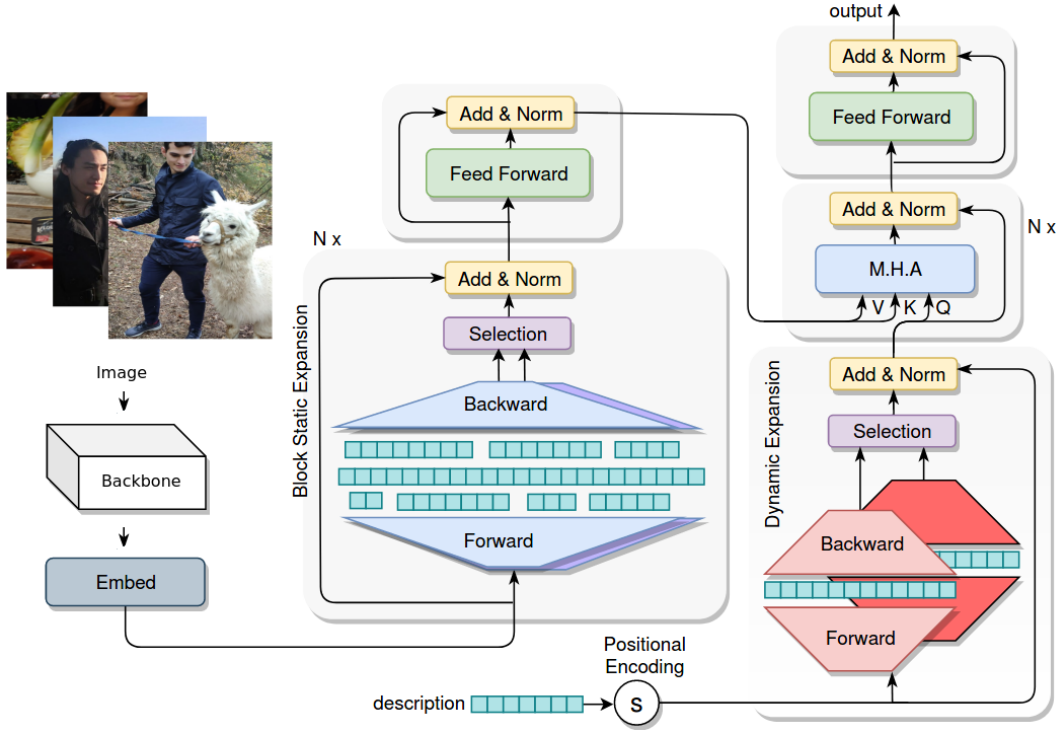


Figure 2: ExpansionNet v2 architecture.

the expanded sequence regardless of the input sequence length L (despite what the name suggests N_E can be also smaller than L) and it involves two parameter matrices Q_E, B_E of size $N_E \times d_m$ called expansion queries and biases respectively. Whereas, in the Dynamic Expansion, given the input sequence $X = \{x_1, x_2, \dots, x_L\}$ and the expansion factor N_E , considering two parameter matrices $E_Q, E_B \in \mathbb{R}^{N_E \times d_m}$, the expansion queries Q^E and expansion biases B_E are defined by:

$$\begin{aligned} Q_E &= (C^\top \mathbb{H}_E)^\top + (E_Q^\top \mathbb{I}_E)^\top \\ B_E &= (C^\top \mathbb{H}_E)^\top + (E_B^\top \mathbb{I}_E)^\top \end{aligned} \quad (4)$$

where $C \in \mathbb{R}^{L \times d_m}$ defines a linear projection of the input and $H_E \in \mathbb{R}^{L \times (L \cdot N_E)}$ is defined as:

$$\mathbb{H}_E = \begin{bmatrix} \mathbf{1} & \mathbf{0} & \dots & \mathbf{0} \\ \mathbf{0} & \mathbf{1} & \dots & \mathbf{0} \\ \vdots & \vdots & \ddots & \vdots \\ \mathbf{0} & \mathbf{0} & \dots & \mathbf{1} \end{bmatrix}, \quad \mathbf{1}, \mathbf{0} \in \mathbb{R}^{1 \times N_E}$$

and $I_E \in \mathbb{R}^{N_E \times (L \cdot N_E)}$ is defined by the column-wise concatenation of L identity matrices of size $N_E \times N_E$:

$$\mathbb{I}_E = [\mathbb{I}_L \quad \mathbb{I}_L \quad \dots \quad \mathbb{I}_L], \quad \mathbb{I}_L \in \mathbb{R}^{N_E \times N_E}$$

The second forward part and the remaining operations involve 4 linear projections $K, V_1, V_2, S \in \mathbb{R}^{L \times d_m}$. First of all, the ‘‘Length Transformation Matrix’’ denoted as M is computed using K and the expanded queries previously generated:

$$M = \frac{Q_E K^\top}{\sqrt{d_m}}. \quad (5)$$

Given row-wise normalization operator $\Psi : (X, \epsilon) \rightarrow Y$, $X, Y \in \mathbb{R}^{N_1 \times N_2}, \epsilon \in \mathbb{R}^+ / \{0\}$:

$$\Psi(X, \epsilon)_{ij} = \frac{x_{ij}}{\sum_{z=1}^{N_2} x_{iz} + \epsilon} \quad (6)$$

where the coefficient ϵ ensures the feasibility of the operation, the forward processing consists of:

$$\begin{aligned} R_i^{fw} &= \Psi(\text{ReLU}((-1)^i M), \epsilon) \quad i \in \{1, 2\} \\ F_i^{fw} &= R_i^{fw} V_i + B_E \quad i \in \{1, 2\} \end{aligned} \quad (7)$$

In the backward step the original sequence length is retrieved back by transposing the length transformation matrix in Equation 5:

$$\begin{aligned} R_i^{bw} &= \Psi(\text{ReLU}((-1)^i M^\top), \epsilon) \quad i \in \{1, 2\} \\ B_i^{bw} &= R_i^{bw} F_i^{fw} \quad i \in \{1, 2\} \end{aligned} \quad (8)$$

Finally the selection phase combine the results produced by the two paths:

$$\text{out} = \sigma(S) \odot B_1^{bw} + (1 - \sigma(S)) \odot B_2^{bw}. \quad (9)$$

In order to increase the effectiveness of the static expansion, we propose an improved version called Block Static Expansion which performs the Forward and Backward operations on a collection of several target lengths instead of one. The layer not only enables the network to leverage a variety of processing perspectives of the input during the features refinement, but eases the hyper parameters exploration as it is more likely to

find the most suitable expansion coefficients for a given problem. From a formulation perspective, the vector generation phase is repeated over a given group of arbitrary number of lengths $G = \{N_E^1, N_E^2, \dots, N_E^{N_G}\}$. Despite the increase of the number of sequence lengths, the number of parameters are not increased thanks to the parameters sharing and it is implemented in a way such that both forward and backward steps are performed over all targets at the same time, in particular the grouped expansion queries and biases are now defined as:

$$\begin{aligned} E_Q^G &= \{(E_Q^1)^\top, (E_Q^2)^\top, \dots, (E_Q^{N_G})^\top\}^\top \\ E_B^G &= \{(E_B^1)^\top, (E_B^2)^\top, \dots, (E_B^{N_G})^\top\}^\top \end{aligned} \quad (10)$$

thus the computational efficiency of the original formulation is preserved. During the backward stage the length transformation matrix is scaled by the inverse number of lengths in each block $\frac{1}{N_G}$.

3.3 Training objectives

The model is first pre-trained using the Cross-Entropy loss L_{XE} :

$$L_{XE}(\theta) = - \sum_t^M \log(p_\theta(y_t^* | y_{1:t-1}^*, I)) \quad (11)$$

where $p_\theta(y_t^* | y_{1:t-1}^*, I)$ is the probability assigned by the model θ to the target y_t^* given the image I and the previous words $y_{1:t-1}^*$. Then the self-critical optimization [26] is performed according the following formula:

$$L_{RF}(\theta) = -(r - b) \cdot \sum_t^M \log(p_\theta(y_t | y_{1:t-1})) \quad (12)$$

where b is the baseline computed according to [22], r is the reward assigned to the sampled sequence referred as $y_{1:M}$ and $y_{1:M}^*$ is the ground truth caption. Although we adopt only two losses, in this work each training stage is split into two additional steps in order to allow a broader number of computational resources to reproduce this work. More details are provided in Section 4.3.

4 Experiments

4.1 Dataset

The training dataset consists of the popular Microsoft COCO benchmark [19] split according to [16] resulting in 113.287 training images and 5000 validation images and 5000 testing cases. Each reference caption is pre-processed by a simple pipeline that consists of lower-casing, punctuation removal and filtering out words that do not occur at least 5 times (vocabulary of size 10.000). Additionally, the final model is evaluated over the Novel Object Captioning at Scale dataset (nocaps)

validation set [1] which consists of three class of images called in-domain, near-domain and out-domain, according to the familiarity of the classes with respect to those contained in the training set. This dataset is subject to the same pre-processing of MS-COCO and serves the purpose of further challenging the model in unfavourable conditions.

4.2 Model details

Three models are implemented for the experiment results. Each one rely on top of the same backbone, the Swin-Transformer in the Large configuration [21] pre-trained on ImageNet [8]. All images are subject to a minimal pre-processing: first they are resized into a $3 \times 384 \times 384$ tensor, then RGB values are converted into a $[0, 1]$ range and further normalized using $mean=(0.485, 0.456, 0.406)$ and $std=(0.229, 0.224, 0.225)$. The baseline, which is the Base Transformer, and our main model, referred as "ExpansionNet v2", are implemented with the following configurations $d_m=512$, $d_{ff}=2048$, $N_{enc}=N_{dec}=3$. In the latter, the dynamic expansion coefficients is set to 16 and the improved static expansion coefficients consist of $G=\{32, 64, 128, 256, 512\}$ (more details in Section 4.4).

Table 1: Comparison between our training strategy and the standard one using a single Nvidia A100 GPU.

Training	Standard	Ours	Speed-up
Cross-Entropy	10 days	1.5 days	6.7
Reinforcement	5 days	1 day	5
Complete	15 days	2.5 days	6

4.3 Training algorithm

From the sheer number of parameters perspective alone it can be observed that the Swin-Transformer backbone is the biggest part of the system, hence it represents the most computationally expensive portion of the training phase. Following this observation, in order to enable the end-to-end training step to a broader number of computational architectures, our training is divided in four steps, in particular each phase, during either the pre-training and the reinforcement stages, consists of an initial training in which the backbone's weights are freezed and a fine-tuning step during which gradients flow throughout the whole system:

1. **Cross-Entropy – Freezed backbone.** The model is trained using batch size 48, an initial learning rate of $2e-4$, a warmup of 10.000 and is annealed by 0.8 every 2 epochs for 8 epochs;
2. **Cross Entropy – End to end.** The whole system is trained for 2 additional epochs, using batch size 48 and an initial learning rate of $3e-5$ annealed by 0.55 every epoch;

Table 2: Ablation study in the first stage of Cross-Entropy training using beam size 3 over the Karpathy test split.

Encoder	Decoder	B1	B2	B3	B4	M	R	C	S
Baseline	Baseline	74.8	58.4	44.8	34.2	28.3	56.7	115.8	21.5
Static Exp. $G=\{64\}$	Dyn. Exp.	76.9	61.1	47.5	36.6	28.8	57.6	121.9	22.3
Static Exp $G=\{128, 128, 128, 128, 128\}$	Dyn. Exp.	76.4	60.8	47.2	36.5	29.2	57.8	122.6	22.6
Static Exp $G=\{384, 384, 384, 384, 384\}$	Dyn. Exp.	77.3	61.4	47.8	36.8	29.1	57.9	122.7	22.6
Static Exp $G=\{512, 512, 512, 512, 512\}$	Dyn. Exp.	76.9	60.9	47.1	36.1	29.2	57.6	122.9	22.7
Static Exp $G=\{8, 16, 32, 64, 96, 128, 256\}$	Dyn. Exp.	77.1	61.4	47.6	36.5	29.0	57.8	123.0	22.5
Static Exp $G=\{16, 32, 64, 128, 196, 256, 320\}$	Dyn. Exp.	77.0	61.2	47.6	36.6	29.2	57.7	123.3	22.6
Static Exp $G=\{128, 256, 384, 512\}$	Dyn. Exp.	77.4	61.6	47.8	36.8	29.1	57.8	123.4	22.6
Static Exp. $G=\{32, 64, 128, 256, 512\}$	Dyn. Exp.	77.4	61.6	47.8	36.8	29.3	58.0	123.8	22.7

3. CIDEr-D optimization – Freezed backbone.

Reinforcement phase adopt a batch size of 48, an initial learning rate of 1e-4, no warmup, annealed by 0.8 every epoch for 9 epochs;

4. CIDEr-D optimization – End to end.



The whole system is fine-tuned for few more iterations up to an additional epoch using a batch size of 48 and fixed learning rate 2e-6. This step is optional since it only slightly contribute to the final performances and can be skipped in case no improvements are observed.

Despite its apparent complexity, it is much more computational friendly compared to the standard method consisting of a small batch size of 10 for 30 epochs for both optimization steps. As a matter of fact, only a much smaller number of training epochs are dedicated for the fine-tuning of the whole system. This not only means that most of the time the cost of computing the required information related to backbone’s gradient is avoided, but the cost of the forward operation can be drastically reduced as well. In particular, in our implementation, during step 1 and 3 the backbone’s forward pass is performed only once for each image in the data set therefore the forward cost is replaced by a memory read and copy. This configuration not only results in a significant decrease of the training time, as show in Table 1, but it is able to achieve even higher performances compared to the end-to-end training showcased in [33] (see Table 4). All steps are trained using the RAdam optimizer [20] ($\beta_1 = 0.9$, $\beta_2 = 0.98$).

4.4 Ablation Study

In Table 2 we compare the results of the improved Static Expansion over the previous one. We adopt several configurations covering a wide range of lengths. First of all, there is no apparent relation between the size of the length groups and the performance, as more targets does not necessarily yield better performances, in contrast to the diversity, where instances like $\{128, 128, 128, 128, 128\}$, $\{256, 256, 256, 256, 256\}$ and $\{512, 512, 512, 512, 512\}$ lead to a less significant increase in performance compared to $\{8, 16, 32, 64, 96, 128, 256\}$ or $\{16, 32, 64, 128, 196, 256, 320\}$. The most successful configuration in terms of CIDEr, which will

Table 3: Two examples of captions sampled from the Karpathy test split.

Image	Captions
	<p>Baseline: A cat looking in front of a mirror.</p> <p>ExpansionNet v2: A cat looking at its reflection in a mirror.</p> <p>Gt: { A cat looking at his reflection in the mirror. ; A cat that is looking in a mirror. ; A cat looking at itself in a mirror. ; A cat looking at itself adoringly in a mirror. ; A cat stares at itself in a mirror. }</p>
	<p>Baseline: A cat on a leash next to a water bottle.</p> <p>ExpansionNet v2: Two pictures of a cat and a dog on a leash.</p> <p>Gt: { A gray and white cat sitting on top of a table. ; A double picture with one featuring a dog and the other a cat. ; A dog is shown above a cat picture, A dog and cat in a coupe of photos. ; Two pictures of a dog and a cat sitting. }</p>

be adopted in the remaining experiments, is $\{32, 64, 128, 256, 512\}$ and it suggests that in addition to the diversity, the model benefits from adopting both short and long expansion sequences. For instance, removing either the smallest or greatest end from the targets length interval, like in the case of $\{128, 256, 384, 512\}$, leads to a performance downgrade. Remarkably, all instances perform better than the baseline across all metrics.

4.5 Performance comparison

COCO Offline Evaluation. Table 4 reports the score comparison between ExpansionNet v2 and the best performing models in recent years. Up-Down [3] introduced the idea of extracting a collection of features from the images using an object detector like Faster-RCNN [25] in contrast to the classification backbone [35]. The idea was adopted in most of the

Table 4: Offline comparison of state of art models over the Karpathy test split.

Model	Cross-Entropy						CIDEr-D optimization					
	B@1	B@4	M	R	C	S	B@1	B@4	M	R	C	S
Single Model												
Up-Down [3]	77.2	36.2	27.0	56.4	113.5	20.3	79.8	36.3	27.7	56.9	120.1	21.4
GCN-LSTM [38]	77.3	36.8	27.9	57.0	116.3	20.9	80.5	38.2	28.5	58.3	127.6	22.0
SGAE [36]	-	-	-	-	-	-	80.8	38.4	28.4	58.6	127.8	22.1
AoANet [13]	77.4	37.2	28.4	57.5	119.8	21.3	80.2	38.9	29.2	58.8	129.8	22.4
X-Transformer [24]	77.3	37.0	28.7	57.5	120.0	21.8	80.9	39.7	29.5	59.1	132.8	23.4
GET [15]	-	-	-	-	-	-	81.5	39.5	29.3	58.9	131.6	22.8
DLCT [23]	-	-	-	-	-	-	81.4	39.8	29.5	59.1	133.8	23.0
RSTNet [40]	-	-	-	-	-	-	81.8	40.1	29.8	59.5	135.6	23.3
PureT [33]	-	-	-	-	-	-	82.1	40.9	30.2	60.1	138.2	24.2
ExpansionNet v2	78.1	38.1	30.1	58.9	128.2	23.5	82.8	41.5	30.3	60.5	140.4	24.5
Ensemble Model												
GCN-LSTM [38]	77.4	37.1	28.1	57.2	117.1	21.1	80.9	38.3	28.6	58.5	128.7	22.1
SGAE [36]	-	-	-	-	-	-	81.0	39.0	28.4	58.9	129.1	22.2
AoANet [13]	78.7	38.1	28.5	58.2	122.7	21.7	81.6	40.2	29.3	59.4	132.0	22.8
X-Transformer [24]	77.8	37.7	29.0	58.0	122.1	21.9	81.7	40.7	29.9	59.7	135.3	23.8
GET [15]	-	-	-	-	-	-	82.1	40.6	29.8	59.6	135.1	23.8
DLCT [23]	-	-	-	-	-	-	82.2	40.8	29.9	59.8	137.5	23.3
PureT [33]	-	-	-	-	-	-	83.4	42.1	30.4	60.8	141.0	24.3
ExpansionNet v2	78.5	38.5	29.9	58.8	128.7	23.6	83.5	42.7	30.6	61.1	143.7	24.7

Table 5: Online server results on the MS-COCO 2014 test set which ground truth are unknown.

Model	B1		B2		B3		B4		METEOR		ROUGE-L		CIDEr-D	
	c5	c40	c5	c40	c5	c40	c5	c40	c5	c40	c5	c40	c5	c40
SCST [26]	78.1	93.7	61.9	86.0	47.0	75.9	35.2	64.5	27.0	35.5	56.3	70.7	114.7	116.0
Up-Down [3]	80.2	95.2	64.1	88.8	49.1	79.4	36.9	68.5	27.6	36.7	57.1	72.4	117.9	120.5
GCN-LSTM [38]	-	-	65.5	89.3	50.8	80.3	38.7	69.7	28.5	37.6	58.5	73.4	125.3	126.5
SGAE [36]	81.0	95.3	65.6	89.5	50.7	80.4	38.5	69.7	28.2	37.2	58.6	73.6	123.8	126.5
AoANet [13]	81.0	95.0	65.8	89.6	51.4	81.3	39.4	71.2	29.1	38.5	58.9	74.5	126.9	129.6
X-Transformer [24]	81.9	95.7	66.9	90.5	52.4	82.5	40.3	72.4	29.6	39.2	59.5	75.0	131.1	133.5
RSTNet [40]	82.1	96.4	67.0	91.3	52.2	83.0	40.0	73.1	29.6	39.1	59.5	74.6	131.9	134.0
GET [15]	81.6	96.1	66.5	90.9	51.9	82.8	39.7	72.9	29.4	38.8	59.1	74.4	130.3	132.5
DLCT [23]	82.4	96.6	67.4	91.7	52.8	83.8	40.6	74.0	29.8	39.6	59.8	75.3	133.3	135.4
PureT [33]	82.8	96.5	68.1	91.8	53.6	83.9	41.4	74.1	30.1	39.9	60.4	75.9	136.0	138.3
ExpansionNet v2	83.3	96.9	68.8	92.6	54.4	85.0	42.1	75.3	30.4	40.1	60.8	76.4	138.5	140.8

following architectures as well, for instance in case of GCN-LSTM [38] and SGAE [36], which, additionally, implemented a graph convolutional network on top of it in order to exploit the information provided by a scene graph. AoANet [13] instead, relied on a Transformer based architecture and improved the attentive components with two gates serving the purpose of simulating an additional level of attention over the inputs and augmented the language modeling part with a LSTM. X-Transformer [24] on the other hand, adopted a fully attentive architecture and further refined the attentive blocks by means of bilinear pooling techniques. The most recent and performing architectures redefined the best way of feeding the visual input into the network, for instance RSTNet [40] showcased the effectiveness of grid features over regions, GET [15] processed the images using a global representation as well in addition to the local ones, DLCT [23] instead exploited the advantages of both regions and grid visual features. Finally PureT [33] removed the convolutional backbone and implemented an entirely attentive model based upon the novel Swin-Transformer, hence applying Window

/ Shifted-Window MHA in both encoder and decoder. ExpansionNet v2 outperforms all the previous models across all metrics in both single and ensemble configuration, in particular it achieves the new state of art performance, outperforming the previous one by 0.1 BLEU1, 0.6 BLEU4, 0.3 ROUGE-L, 2.7 CIDEr-D and 0.4 SPICE in the ensemble configuration.

COCO Online Evaluation. We evaluate ExpansionNet v2 using the ensemble configuration and adopting the standard Beam Search (beam size 5) over the official testing set of 40.775 images, submitting the predictions to the online testing server. Results are reported in Table 5, c5 and c40 represent the scores in case of 5 and 40 reference captions (unknown to the user) respectively. Similarly to the offline case, it achieves the new state of art performance across all metrics (2 July 2022), in particular it outperforms the previous best performing model by a margin of 1.2 BLEU4 (c40), 0.2 METEOR (c40), 0.5 ROUGE-L (c40) and 2.5 CIDEr-D in both c5 and c40 instances.



Figure 3: Attention visualization of one head in one of our main model layers.

Table 6: Performances comparison on nocaps validation set.

Domain	Metric	Enc-Dec[5]	Up-Down[3]	Ours
In	C	72.8	78.1	83.8
	S	11.1	11.6	12.6
Near	C	57.1	57.7	79.2
	S	10.2	10.3	12.4
Out	C	34.1	31.3	54.0
	S	8.3	8.3	9.3
All	C	54.7	55.3	72.9
	S	10.0	10.1	11.4

Table 7: Three examples of nocaps out-of-domain images, for the sake of brevity only 3 ground truth descriptions are reported.

Image	Captions
	<p>Pred: A close up of a fish in a body of water.</p> <p>Gt: { A seahorse in an aquarium full of water with some plants growing in the background. ; A blue seahorse is swimming near sea plants on back. ; A very small seahorse is in the water along with other pieces. }</p>
	<p>Pred: Three pictures of a blender with red liquid in it.</p> <p>Gt: { A picture of three blenders with a strawberry looking beverage inside. ; A white mixer in the process of making a smoothie. ; The steps of making a smoothie in a blender are shown. }</p>
	<p>Pred: A birthday cake is decorated with a house.</p> <p>Gt: { A gingerbread house has a red frosting roof and several candy pieces. ; A gingerbread house that is red, brown, white, and green. ; A log cabin is made out of dessert treats. }</p>

Nocaps Evaluation. We evaluate ExpansionNet v2 over the nocaps validation set. In particular, we adopt a single model trained exclusively on Cross-Entropy Loss, using no additional pre-training data sets and the predictions are generated by the standard Beam Search

algorithm (beam size 3) in contrast to the CBS [2]. A limited comparison is reported in Table 6 which shows cases that our model achieves very competitive results among the architectures trained in similar configurations, with a overall lead of 17.6 CIDEr and 1.4 SPICE over the Up-Down model [3]. However, it’s worth noting that it is still ultimately outperformed by many recent works such as [12, 39, 17, 18] which results are omitted because of a different experiment setup.

4.6 Qualitative Analysis

Table 8 and 9 provide some examples of captions. Regardless of the complexity, ExpansionNet v2 appears not only able to correctly describe the subjects depicted in the scenes but also showcases a good level of semantic understanding by describing also the goals and interactions (Images 1, 8 and 12). Unfortunately, our model seem to struggle with out-of-domain objects as showcased in Table 7 where, because of objects and terms unknown to the model, predictions are either imprecise (2nd image) or incorrect (1st and 3rd image). Nonetheless, it seems to be able of providing a rough description of the images context. Finally, we showcase an example of attention visualization in Figure 3, despite the absence of an object detector, the scattered focus correctly outlines the main subjects.

5 Conclusion

We presented a novel architecture for image captioning based upon the expansion methods and in particular the Block Static Expansion enabling the model to process sequences in multiple different forms each one defined by an arbitrary number of elements in contrast to the one provided by the input, which ultimately increases the quality of features refinement. To support this claim we implemented an end to end encoder-decoder architecture called ExpansionNet v2 which parameters are found by means of an alternating full and partial end-to-end training strategy. Experiments conducted over the COCO and nocaps dataset resulted in the new state of art performance in the first and very competitive results for the latter.

Bibliography

- [1] Harsh Agrawal, Karan Desai, Yufei Wang, Xinlei Chen, Rishabh Jain, Mark Johnson, Dhruv Batra, Devi Parikh, Stefan Lee, and Peter Anderson. “Nocaps: Novel object captioning at scale”. In: *Proceedings of the IEEE/CVF International Conference on Computer Vision*. 2019, pp. 8948–8957.
- [2] Peter Anderson, Basura Fernando, Mark Johnson, and Stephen Gould. “Guided open vocabulary image captioning with constrained beam search”. In: *arXiv preprint arXiv:1612.00576* (2016).
- [3] Peter Anderson, Xiaodong He, Chris Buehler, Damien Teney, Mark Johnson, Stephen Gould, and Lei Zhang. “Bottom-up and top-down attention for image captioning and visual question answering”. In: *Proceedings of the IEEE conference on computer vision and pattern recognition*. 2018, pp. 6077–6086.
- [4] Dzmitry Bahdanau, Kyunghyun Cho, and Yoshua Bengio. “Neural machine translation by jointly learning to align and translate”. In: *arXiv preprint arXiv:1409.0473* (2014).
- [5] Soravit Changpinyo, Piyush Sharma, Nan Ding, and Radu Soricut. “Conceptual 12m: Pushing web-scale image-text pre-training to recognize long-tail visual concepts”. In: *Proceedings of the IEEE/CVF Conference on Computer Vision and Pattern Recognition*. 2021, pp. 3558–3568.
- [6] Kyunghyun Cho, Bart Van Merriënboer, Caglar Gulcehre, Dzmitry Bahdanau, Fethi Bougares, Holger Schwenk, and Yoshua Bengio. “Learning phrase representations using RNN encoder-decoder for statistical machine translation”. In: *arXiv preprint arXiv:1406.1078* (2014).
- [7] Chaorui Deng, Ning Ding, Minghui Tan, and Qi Wu. “Length-controllable image captioning”. In: *European Conference on Computer Vision*. Springer. 2020, pp. 712–729.
- [8] Jia Deng, Wei Dong, Richard Socher, Li-Jia Li, Kai Li, and Li Fei-Fei. “Imagenet: A large-scale hierarchical image database”. In: *2009 IEEE conference on computer vision and pattern recognition*. Ieee. 2009, pp. 248–255.
- [9] Simao Herdade, Armin Kappeler, Kofi Boakye, and Joao Soares. “Image captioning: Transforming objects into words”. In: *arXiv preprint arXiv:1906.05963* (2019).
- [10] Sepp Hochreiter and Jürgen Schmidhuber. “Long short-term memory”. In: *Neural computation* 9.8 (1997), pp. 1735–1780.
- [11] Jia Cheng Hu. “ExpansionNet: exploring the sequence length bottleneck in the Transformer for Image Captioning”. In: *arXiv preprint arXiv:2207.03327* (2022).
- [12] Xiaowei Hu, Zhe Gan, Jianfeng Wang, Zhengyuan Yang, Zicheng Liu, Yumao Lu, and Lijuan Wang. “Scaling up vision-language pre-training for image captioning”. In: *Proceedings of the IEEE/CVF Conference on Computer Vision and Pattern Recognition*. 2022, pp. 17980–17989.
- [13] Lun Huang, Wenmin Wang, Jie Chen, and Xiao-Yong Wei. “Attention on attention for image captioning”. In: *Proceedings of the IEEE International Conference on Computer Vision*. 2019, pp. 4634–4643.
- [14] Zhiheng Huang, Peng Xu, Davis Liang, Ajay Mishra, and Bing Xiang. “TRANS-BLSTM: Transformer with bidirectional LSTM for language understanding”. In: *arXiv preprint arXiv:2003.07000* (2020).
- [15] Jiayi Ji, Yunpeng Luo, Xiaoshuai Sun, Fuhai Chen, Gen Luo, Yongjian Wu, Yue Gao, and Rongrong Ji. “Improving image captioning by leveraging intra-and inter-layer global representation in transformer network”. In: *Proceedings of the AAAI conference on artificial intelligence*. Vol. 35. 2. 2021, pp. 1655–1663.
- [16] Andrej Karpathy and Li Fei-Fei. “Deep visual-semantic alignments for generating image descriptions”. In: *Proceedings of the IEEE conference on computer vision and pattern recognition*. 2015, pp. 3128–3137.
- [17] Junnan Li, Dongxu Li, Caiming Xiong, and Steven Hoi. “Blip: Bootstrapping language-image pre-training for unified vision-language understanding and generation”. In: *arXiv preprint arXiv:2201.12086* (2022).
- [18] Xiujun Li, Xi Yin, Chunyuan Li, Pengchuan Zhang, Xiaowei Hu, Lei Zhang, Lijuan Wang, Houdong Hu, Li Dong, Furu Wei, et al. “Oscar: Object-semantics aligned pre-training for vision-language tasks”. In: *European Conference on Computer Vision*. Springer. 2020, pp. 121–137.
- [19] Tsung-Yi Lin, Michael Maire, Serge Belongie, James Hays, Pietro Perona, Deva Ramanan, Piotr Dollár, and C Lawrence Zitnick. “Microsoft coco: Common objects in context”. In: *European conference on computer vision*. Springer. 2014, pp. 740–755.
- [20] Liyuan Liu, Haoming Jiang, Pengcheng He, Weizhu Chen, Xiaodong Liu, Jianfeng Gao, and Jiawei Han. “On the variance of the adaptive learning rate and beyond”. In: *arXiv preprint arXiv:1908.03265* (2019).

- [21] Ze Liu, Yutong Lin, Yue Cao, Han Hu, Yixuan Wei, Zheng Zhang, Stephen Lin, and Baining Guo. “Swin transformer: Hierarchical vision transformer using shifted windows”. In: *Proceedings of the IEEE/CVF International Conference on Computer Vision*. 2021, pp. 10012–10022.
- [22] Ruotian Luo. “A Better Variant of Self-Critical Sequence Training”. In: *arXiv preprint arXiv:2003.09971* (2020).
- [23] Yunpeng Luo, Jiayi Ji, Xiaoshuai Sun, Liujuan Cao, Yongjian Wu, Feiyue Huang, Chia-Wen Lin, and Rongrong Ji. “Dual-level collaborative transformer for image captioning”. In: *Proceedings of the AAAI Conference on Artificial Intelligence*. Vol. 35. 3. 2021, pp. 2286–2293.
- [24] Yingwei Pan, Ting Yao, Yehao Li, and Tao Mei. “X-Linear Attention Networks for Image Captioning”. In: *Proceedings of the IEEE/CVF Conference on Computer Vision and Pattern Recognition*. 2020, pp. 10971–10980.
- [25] Shaoqing Ren, Kaiming He, Ross Girshick, and Jian Sun. “Faster r-cnn: Towards real-time object detection with region proposal networks”. In: *arXiv preprint arXiv:1506.01497* (2015).
- [26] Steven J Rennie, Etienne Marcheret, Youssef Mroueh, Jerret Ross, and Vaibhava Goel. “Self-critical sequence training for image captioning”. In: *Proceedings of the IEEE Conference on Computer Vision and Pattern Recognition*. 2017, pp. 7008–7024.
- [27] Zhan Shi, Xu Zhou, Xipeng Qiu, and Xiaodan Zhu. “Improving image captioning with better use of captions”. In: *arXiv preprint arXiv:2006.11807* (2020).
- [28] Richard Socher and Li Fei-Fei. “Connecting modalities: Semi-supervised segmentation and annotation of images using unaligned text corpora”. In: *2010 IEEE Computer Society Conference on Computer Vision and Pattern Recognition*. IEEE. 2010, pp. 966–973.
- [29] Ashish Vaswani, Noam Shazeer, Niki Parmar, Jakob Uszkoreit, Llion Jones, Aidan N Gomez, Łukasz Kaiser, and Illia Polosukhin. “Attention is all you need”. In: *Advances in neural information processing systems*. 2017, pp. 5998–6008.
- [30] Oriol Vinyals, Alexander Toshev, Samy Bengio, and Dumitru Erhan. “Show and tell: A neural image caption generator”. In: *Proceedings of the IEEE conference on computer vision and pattern recognition*. 2015, pp. 3156–3164.
- [31] Chaoyang Wang, Ziwei Zhou, and Liang Xu. “An integrative review of image captioning research”. In: *journal of physics: conference series*. Vol. 1748. 4. IOP Publishing. 2021, p. 042060.
- [32] Li Wang, Zechen Bai, Yonghua Zhang, and Hongtao Lu. “Show, Recall, and Tell: Image Captioning with Recall Mechanism”. In: *Proceedings of the AAAI Conference on Artificial Intelligence*. Vol. 34. 07. 2020, pp. 12176–12183.
- [33] Yiyu Wang, Jungang Xu, and Yingfei Sun. “End-to-End Transformer Based Model for Image Captioning”. In: *arXiv preprint arXiv:2203.15350* (2022).
- [34] Ruibin Xiong, Yunchang Yang, Di He, Kai Zheng, Shuxin Zheng, Chen Xing, Huishuai Zhang, Yanyan Lan, Liwei Wang, and Tieyan Liu. “On layer normalization in the transformer architecture”. In: *International Conference on Machine Learning*. PMLR. 2020, pp. 10524–10533.
- [35] Kelvin Xu, Jimmy Ba, Ryan Kiros, Kyunghyun Cho, Aaron Courville, Ruslan Salakhudinov, Rich Zemel, and Yoshua Bengio. “Show, attend and tell: Neural image caption generation with visual attention”. In: *International conference on machine learning*. 2015, pp. 2048–2057.
- [36] Xu Yang, Kaihua Tang, Hanwang Zhang, and Jianfei Cai. “Auto-encoding scene graphs for image captioning”. In: *Proceedings of the IEEE/CVF Conference on Computer Vision and Pattern Recognition*. 2019, pp. 10685–10694.
- [37] Benjamin Z Yao, Xiong Yang, Liang Lin, Mun Wai Lee, and Song-Chun Zhu. “I2t: Image parsing to text description”. In: *Proceedings of the IEEE* 98.8 (2010), pp. 1485–1508.
- [38] Ting Yao, Yingwei Pan, Yehao Li, and Tao Mei. “Exploring visual relationship for image captioning”. In: *Proceedings of the European conference on computer vision (ECCV)*. 2018, pp. 684–699.
- [39] Pengchuan Zhang, Xiujun Li, Xiaowei Hu, Jianwei Yang, Lei Zhang, Lijuan Wang, Yejin Choi, and Jianfeng Gao. “Vinvl: Making visual representations matter in vision-language models”. In: (2021).
- [40] Xuying Zhang, Xiaoshuai Sun, Yunpeng Luo, Jiayi Ji, Yiyi Zhou, Yongjian Wu, Feiyue Huang, and Rongrong Ji. “RSTNet: Captioning with adaptive attention on visual and non-visual words”. In: *Proceedings of the IEEE/CVF conference on computer vision and pattern recognition*. 2021, pp. 15465–15474.

Table 8: Examples of captions in single model configuration (beam search 5).




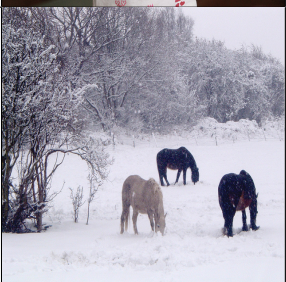
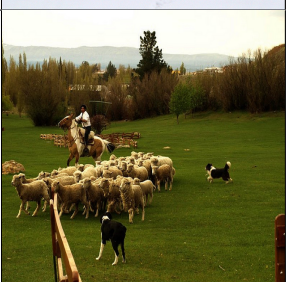







Id	Image	Networks prediction	Ground Truth
1		Baseline: A man holding a tennis ball on a tennis court. ExpansionNet v2: A man jumping in the air to hit a tennis ball.	Gt1: A tennis player jumps and swats at the ball. Gt2: A tennis player hitting a tennis ball on a court. Gt3: Professional tennis player immediately after returning a shot. Gt4: A man with a tennis racket plays a game of tennis. Gt5: A man playing tennis with two people watching the game.
2		Baseline: A giraffe standing next to a man in a field. ExpansionNet v2: A giraffe eating from a feeder in a park.	Gt1: A giraffe sticking its head in a feeding basket with trees in background. Gt2: Giraffe reaching into basket with trees in background. Gt3: A very tall adult giraffe eating from a basket. Gt4: A giraffe is eating out of a basket. Gt5: A giraffe eating from a man made feeder.
3		Baseline: A little girl brushing her hair with a table. ExpansionNet v2: A little girl brushing her hair with a pink brush.	Gt1: A young girl tries to comb her own hair. Gt2: A young child brushing her hair with a big pink brush. Gt3: A young girl is trying to brush her hair with a pink brush. Gt4: A little girl with a bunny shirt brushing her hair with a pink brush. Gt5: A young girl is combing her hair and looking at the camera.
4		Baseline: Three horses grazing in the snow with a sheep. ExpansionNet v2: Three horses grazing in the snow in a field.	Gt1: Two brown horses standing next to a white horse on a snow covered field. Gt2: A group of horses grazing in the snow. Gt3: Horses eating grass through the snow in a field. Gt4: Three horses are grazing in the snow covered pasture. Gt5: Three horses grazing in the snow with trees in the background.
5		Baseline: A man riding a horse next to a herd of sheep. ExpansionNet v2: A man on a horse and a dog in a field with a herd of sheep.	Gt1: A herd of sheep walking across green grass. Gt2: A person on a horse is riding near dogs and sheep. Gt3: A man on a horse corralling sheep with his two dogs. Gt4: A rancher and two dogs corralling a herd of sheep. Gt5: A man and two dogs gathering a herd of sheep.
6		Baseline: A dog and a bike standing next to a bicycle. ExpansionNet v2: Two dogs walking down a sidewalk next to a bike.	Gt1: Two small dogs on a sidewalk near a bicycle. Gt2: Two small dogs walk next to a bicycle. Gt3: Two dogs are confronting each other near a parked bicycle. Gt4: A couple small dogs walking next to a bike. Gt5: A pair of dogs on a sidewalk next to a bicycle.

Table 9: More examples.

Id	Image	Networks prediction	Ground Truth
7		Baseline: A bird is sitting in the water. ExpansionNet v2: A large bird swimming in the middle of a body of water.	Gt1: A large bird floating out in the water. Gt2: A bird swimming in wavy water, with a island in the background. Gt3: A pelican stands alone in the middle of the ocean. Gt4: There is a large seagull that is swimming in the water. Gt5: A bird is sitting out on the water.
8		Baseline: A woman taking a picture of a bathroom mirror. ExpansionNet v2: A woman taking a picture of herself in a bathroom mirror.	Gt1: A woman is taking a selfie in her bathroom mirror. Gt2: A curly haired girl with glasses takes a selfie in front of the mirror. Gt3: A woman takes a selfie with her phone in the bathroom mirror. Gt4: Woman in green and maroon shirt taking a picture of herself. Gt5: A person in front of a mirror with a cell phone.
9		Baseline: A bowl of rice and vegetables on a table. ExpansionNet v2: A plastic container of food with vegetables on a table.	Gt1: A white container filled with lots of food. Gt2: A dish of very tasty looking food with some veggies. Gt3: Assorted food items displayed in white dish on wooden table. Gt4: A plate full of food including: broccoli, quinoa, black beans and vegetables. Gt5: A bowl full of food, including broccoli and corn.
10		Baseline: A group of donuts sitting on top of a coffee. ExpansionNet v2: A picture of two donuts and a cup of coffee.	Gt1: A cook book for making donuts with donuts and coffee pictures on it's cover. Gt2: A picture of glazed donuts and coffee on a table. Gt3: A Spanish advertisement for two sweet glazed donuts. Gt4: A sign is describing delicious glazed donuts on a napkin. Gt5: Two doughnuts on a napkin next to a cup of tea and a Spanish ad.
11		Base: A woman sitting on a bench. ExpansionNet v2: A young girl sitting on a skateboard.	Gt1: Cute girl sitting on a skateboard in the driveway. Gt2: A girl sitting on a skateboard in the driveway. Gt3: A girl is sitting on a skateboard outside. Gt4: A girl is sitting on the sidewalk on her skateboard. Gt5: A girl in an orange sweater is sitting on a skateboard.
12		Baseline: A dog jumping in the air with a frisbee. ExpansionNet v2: A dog jumping in the air to catch a frisbee.	Gt1: A dog catching a Frisbee in the grass. Gt2: The black and white dog just got the frisbee. Gt3: A dog in a vest catching a frisbee. Gt4: a dig jumps in the air to catch a frisbe. Gt5: Dog wearing blue vest catching red flying disc at outdoor event.